In Situ Optical Detection for Ultrasonic Characterization of Materials in a Mach 10 Hypersonic Wind Tunnel

Jordan S. Lum,[1,*] Lionel T. Keene,[1] Benjamin M. Goldberg,[1] Erik Busby,[1] Aric C. Rousso,[1] Brett F. Bathel,[2] Joshua M. Weisberger,[2] Gregory M. Buck,[2] David M. Stobbe,[1] and James S. Stolken[1]

[1] *Lawrence Livermore National Laboratory, Livermore, California 94550, USA*
[2] *NASA Langley Research Center, Hampton, Virginia 23681, USA*

(Received 26 April 2022; revised 10 August 2022; accepted 12 September 2022; published 26 October 2022)

We present results of *in situ* optical detection of ultrasonic waves generated in stainless steel and graphite samples mounted in a flat plate model during hypersonic flow in the 31-Inch Mach 10 wind tunnel at NASA Langley Research Center. Longitudinal waves are excited in the stainless steel and graphite sample inserts by using a contact piezoelectric transducer and the normal displacement on the surface of the sample, exposed to hypersonic fluid flow, is measured optically using a Sagnac interferometer. Measurements are consistent at different Reynolds numbers both with and without a turbulent trip strip present. Additionally, optical detection of laser-generated surface acoustic waves in a stainless-steel sample during flow is presented. These results are a demonstration of laser-based ultrasonics as an *in situ* material characterization technique in hypersonic flow, enabling potential applications of *in situ* monitoring of defect initialization and morphology in hypersonic environments.

DOI: 10.1103/PhysRevApplied.18.044062

I. INTRODUCTION

Laser-based ultrasonics (LBUs) is an all-optical materials evaluation technique currently used in various application areas [1–6]. Commonly, a pulsed laser irradiates the material to generate ultrasound waves due to optical absorption and rapid thermoelastic expansion or ablation that occurs at the material surface [7,8]. A laser interferometer is then used to measure the surface displacement or velocity due to the induced ultrasonic waves traveling through the material [9,10]. Monitoring how the ultrasonic waves reflect and scatter within the material allows for characterizing different features, such as material elastic constants [11], sample thickness [12], or the presence of subsurface defects [13]. Compared to conventional ultrasonic testing, which requires direct contact of piezoelectric transducers to the sample material, LBU benefits from being an all-optical and remote measurement approach allowing *in situ* application in harsh or inaccessible environments [14,15].

For hypersonic research, LBU could be used as an *in situ* material-characterization technique to monitor the response of materials while exposed to high Mach number flow, which would provide critical information necessary for assessing the performance and failure mechanisms of different materials designed for hypersonic vehicles [16–18]. However, the harsh environment exposes material to significant thermal and mechanical loads from the dynamic and unsteady flow fields, which may complicate the understanding of how the ultrasonic waves propagate within the material. Additionally, LBU requires highly sensitive optical detection to measure the subtle ultrasonic scattering from microscale features. Previous to this study, it was unknown if such a measurement would be possible in a hypersonic environment due to effects such as index of refraction variations in the freestream fluid flow, boundary layer above the sample surface, tunnel-wall boundary layer, and the ambient wind-tunnel noise during operation [19,20]. Therefore, optical detection of ultrasound in materials under hypersonic conditions is the first critical component to realizing a LBU diagnostic in a hypersonic environment and is prioritized in this study.

In this study, we report use of a Sagnac interferometer for optical detection of ultrasonic waves generated in stainless-steel and graphite samples during Mach 10 flow. Verification that ultrasound in the materials could be optically detected through the hypersonic flow was initially demonstrated by exciting ultrasonic waves using contact

*lum21@llnl.gov

piezo transducers glued to the back of the samples. Optical detection of ultrasound is found to be robust under various wind-tunnel conditions and still sensitive enough for detecting the narrow-band MHz surface vibrations generated by the transducers. Finally, optical detection of laser-generated surface acoustic waves in steel is shown during flow.

II. EXPERIMENTAL METHODS

Experiments are conducted at the NASA Langley Research Center's 31-Inch Mach 10 wind tunnel facility [21]. Figure 1(a) shows a diagram of the experimental setup. The hypersonic tunnel is operated at Reynolds numbers of 1.6×10^6 m^{-1}, 3.3×10^6 m^{-1}, and 6.6×10^6 m^{-1} for approximately 12 to 16 s in duration. Machined 304 stainless steel and graphite sample inserts approximately 12.7 mm thick were tested in this study. The 304 stainless-steel material is procured from McMaster-Carr and the graphite is type BG03 from Becker Brothers Graphite Corp. The graphite sample surface is sputter coated with a 100-nm-layer thickness of gold to improve optical reflectivity. Each sample insert is mounted in a flat plate model with a sharp leading edge that is injected into the flow with the sample insert surface at the tunnel centerline [22]. Figure 1(b) shows a schlieren image of the hypersonic flow passing over the flat plate model. The boundary-layer thickness is approximately 10 mm at the center of the image. A trip strip composed of a spanwise array of 3-mm-tall diamond pins is also installed approximately 89-mm downstream of the leading edge for several test runs to promote more growth and thickness of the boundary layer prior to passing over the sample insert.

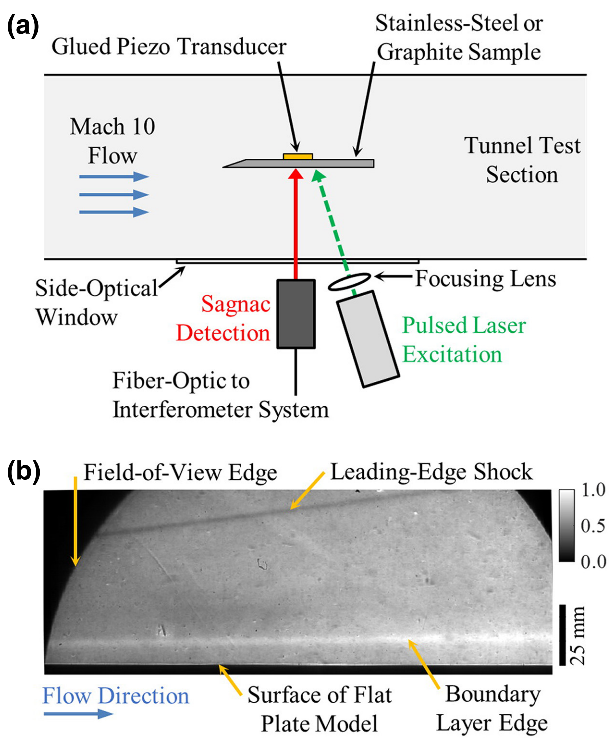

FIG. 1. (a) Diagram of experimental setup. (b) A representative schlieren image with the flat plate model in Mach 10 flow at $\mathrm{Re} = 1.6 \times 10^6$ m^{-1}. Color bar shows normalized pixel intensity.

Optical detection of ultrasonic waves is done using a double differential fiber optic Sagnac interferometer (LuxSonics Inc). More details about this interferometer can be found in the literature [23,24]. Briefly, the Sagnac interferometer is a common-path interferometer that can detect out-of-plane vibration speed of the sample surface using two beams reflected from the same spot on the sample surface. One beam is purposefully phase delayed prior to reaching the sample in order to register surface displacement at a short time after the other beam. After reflection, both beams are made to have no delay between them, and their interference is measured with a balanced photodetector. With both beams passing through the fluid flow, the Sagnac interferometer is potentially less sensitive to changes in the index of refraction from the boundary layer and leading-edge shock compared to a double-path interferometer, which uses a reference beam for interference. Additionally, without the need for a stabilized reference beam and with most of the interferometer system contained in polarization-maintaining optical fibers, the Sagnac interferometer is expected to be less sensitive to environmental vibrations and temperature fluctuations that may be present during wind-tunnel operation.

The Sagnac interferometer uses a 40-mW superluminescent diode that operates in the near-infrared field at 1550-nm wavelength. The probe-beam radiation is emitted from a 50.8-mm diameter telescope detection head with a 500-mm focal length lens, where the output beams reflect off the sample surface and are recollected by the same detection head to couple back into the fiber system. The optical beam diameter FWHM is measured to be approximately 0.1 mm at the focus. The Sagnac interferometer balanced photodetector output (Insight, BPD-1) is sent to a 40-dB preamplifier (Femto, HAS-X-2-40), frequency filtered with a 500-kHz high-pass electrical filter (Thorlabs, EF507) and a 10-MHz low-pass electrical filter (Thorlabs, EF501) to reduce noise, and then recorded on a digital oscilloscope (Tektronix, MSO5104B). FastFrame acquisition on the oscilloscope is used to record several thousand individual time traces, which are later averaged together for enhanced SNR.

To generate ultrasound within the sample materials, either a contact piezo ultrasound transducer (Olympus, V103-RM) or nanosecond pulsed laser (Lumibird, Ultra 20 Stable) is used. The transducers (12.7 mm diameter, 1 MHz center frequency) are glued to the back of each test sample to excite bulk longitudinal waves using a pulser receiver (Panametrics, 1500). The Sagnac interferometer detection spot is aligned epicenter with the piezo transducer on the opposite surface of the sample by maximizing the amplitude of the measured signal output from the interferometer. When the piezo is not used, the pulsed laser is operated at 1064-nm wavelength, 10-ns pulse width, 50-Hz repetition rate, and roughly 14 mJ per pulse. A 500-mm focal length lens is used to focus the pulsed-laser output to a spot size of approximately 1.5 mm FWHM on the sample surface. The pulsed-laser focus is aligned roughly approximately 4 mm away (source-to-receiver distance) from the Sagnac interferometer focus on the sample surface by observing the time of arrival of the surface acoustic wave (SAW) on the oscilloscope as the laser focus is translated closer to the detection spot. For all plotted time traces, time at $t = 0\ \mu$s represents the trigger output of the excitation source from either the pulser receiver that controls the piezo transducer output or the delay generator that controls the q switch of the pulsed laser. Approximately 1 μs of time is purposefully recorded prior to $t = 0\ \mu$s to observe the background noise measured when no ultrasound generation source is present. The ultrasound excitation source (either piezo transducer or pulsed laser) and FastFrame acquisition on the oscilloscope are triggered as the model is injected into the wind tunnel, providing approximately 1-s delay until it reaches centerline in the flow.

III. RESULTS AND DISCUSSION

A. Piezo generation of bulk longitudinal waves in steel

First, to validate the interferometer detection in the hypersonic flow environment, the piezo transducer is used to generate ultrasonic waves reliably and effectively in the sample material. Figures 2(a) and 2(b) show averaged time traces measured using optical detection with piezo generation of bulk longitudinal waves in steel. Piezo excitation occurs at a repetition rate of 1 kHz and time traces are recorded at a sampling rate of 50 MS/sec. Measurements are taken during flow at three different Reynold's numbers with and without a trip strip. Four successive ultrasonic echoes can be seen in each time trace, each representing the time it takes for the ultrasonic wave to travel twice through the thickness of the steel insert. No significant differences are observed between the different runs, indicating the optical detection is not significantly altered by varying flow conditions.

Figure 2(c) shows the rms value for individual time traces recorded from the Sagnac interferometer output during one of the runs. The rms value generally indicates how well focused the interferometer is on the sample surface during the tunnel run duration. The interferometer sensitivity is observed to fluctuate at approximately 12–15 Hz, as shown by the Fourier transform in Fig. 2(d). These fluctuations are later determined to be due to mechanical vibrations of the optical hardware induced by the wind tunnel rather than fluctuations caused by fluid flow [25]. For all Fourier transforms, the mean offset of the time trace is subtracted, a Tukey window is used, and zero-padding is applied (5×10^8 points) before using the MATLAB fast-Fourier-transform function.

Simultaneous detection of the generated ultrasonic waves is also measured by the same piezo transducer

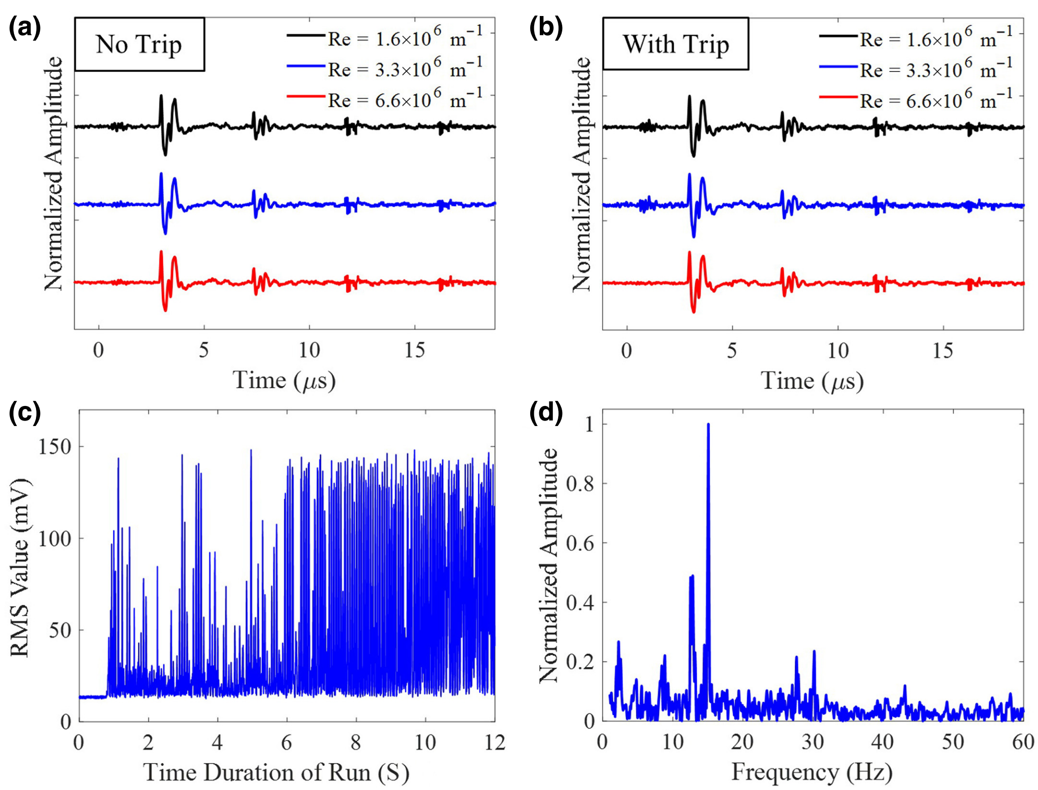

FIG. 2. Averaged time traces of optical detection with piezo excitation on steel during flow with no trip strip (a) and with a trip strip (b). Time traces are normalized and vertically offset for viewing ease. (c) rms of each individual time trace recorded during the test run in part (a) $\mathrm{Re} = 3.3 \times 10^6\ \mathrm{m}^{-1}$. (d) Fourier transform of the RMS trace in (c).

TABLE I. Averaged time of flights calculated from time traces recorded using piezo excitation on the stainless-steel sample with and without flow.

Detection method	Flow condition	Time of flight, μs (mean $\pm$ std. dev.)
Optical	No flow	4.38 ± 0.02
Optical	Flow	4.38 ± 0.02
Piezo	No flow	4.38 ± 0.02
Piezo	Flow	4.38 ± 0.02

TABLE II. Averaged time of flights calculated from time traces recorded using piezo excitation on the graphite sample with and without flow.

Detection method	Flow condition	Time of flight, μs
Optical	No flow	11.45
Optical	Flow	11.50
Piezo	No flow	11.40
Piezo	Flow	11.40

during each run [25]. Additionally, time traces are recorded before wind-tunnel runs (no flow) using both optical and piezo detection methods. The TOF between the first two consecutive ultrasound echoes in all recorded time traces is determined by autocorrelation in MATLAB. The TOF is a quantity of interest for material characterization using ultrasonic testing methods that can be sensitive to material changes, such as thickness [11], elastic properties [11,26], and porosity [27]. The mean TOFs from the two detection methods before and during flow are all in agreement and determined to be 4.38 μs $\pm$ 0.02 μs, as shown in Table I, confirming the Sagnac interferometer can optically detect ultrasonic waves in the steel sample during hypersonic flow.

B. Piezo generation of bulk longitudinal waves in graphite

Figure 3 shows averaged time traces of optical detection and piezo excitation on graphite before and during flow with a trip strip present. Piezo excitation occurs at a repetition rate of 2 kHz and time traces are recorded at a sampling rate of 20 MS/sec. The SNR of the average time trace recorded during flow is found to be too low to accurately quantify a TOF, so a discrete wavelet transform process [25,28–40] is used in MATLAB to empirically denoise the averaged time trace and improve SNR,

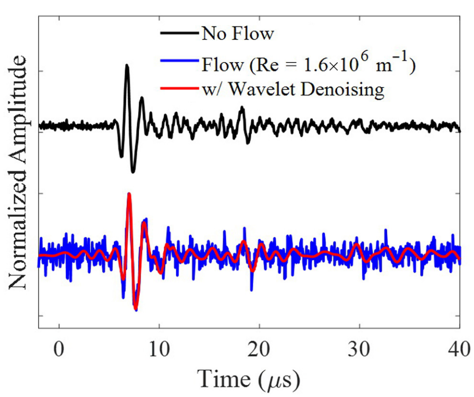

FIG. 3. Averaged time traces of optical detection with piezo excitation on graphite before and during flow with a trip strip. Time traces are normalized and vertically offset for viewing ease.

as shown in Fig. 3. Averaged time trace of piezo detection and excitation on graphite during flow is also recorded.

Table II reports TOFs calculated from the averaged time traces recorded by optical and piezo detection for measurements on graphite before and during flow. There is more variation in the TOF values for graphite than the steel, but these are assumed to be within the uncertainty given the lower measurement sampling rates used for graphite and the higher porosity in graphite, resulting in more scattering of the ultrasonic waves. Nevertheless, the Sagnac interferometer optical detection is confirmed to be able to detect ultrasonic waves in the graphite sample during flow.

C. Laser generation of surface acoustic waves in steel

Figure 4 shows averaged time traces of optical detection and pulsed-laser excitation on steel before and during flow. Pulsed-laser excitation occurs at a repetition rate of 50 Hz and time traces are recorded at a sampling rate of 50 MS/sec. The SAW arrival is detected optically with the Sagnac interferometer during flow. There is a slight increase in the time of arrival of the SAW, or Rayleigh wave, from before to during flow, 1.36 and 1.46 μs, respectively. With a Rayleigh wave speed of approximately 2.85 mm/μs for stainless steel [41], this

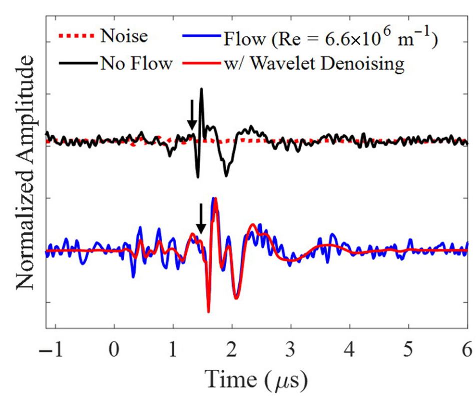

FIG. 4. Averaged time traces of optical detection with pulsed-laser excitation on steel before and during flow with a trip strip. Black arrows point where time of arrival for surface acoustic wave is determined. Time traces are normalized and vertically offset for viewing ease.

could correspond to an increased source-to-receiver distance change of approximately 0.3 mm caused by optical beam steering by the flow. Another possibility could be due to surface heating caused by the flow, which would manifest as a decrease in sound speed [15], and this effect would be more pronounced in the SAW measurement [2] than the through-sample piezo measurement if heating is highly localized to the skin of the material.

IV. CONCLUSION

In conclusion, *in situ* optical detection of ultrasonic waves generated in stainless-steel and graphite samples is successfully measured in a hypersonic environment using a Sagnac interferometer. Optical detection is found to be insensitive to changes in Reynolds number and the relative turbulence of the flow boundary layer. A demonstration of a LBU measurement is also shown in the Mach 10 hypersonic wind tunnel, encouraging future applications of LBU as a suitable method for *in situ* material characterization for hypersonic research.

ACKNOWLEDGMENTS

The diagnostics work is performed under the auspices of the U.S. Department of Energy by Lawrence Livermore National Laboratory under Contract DE-AC52-07NA27344 and is supported by the LLNL-LDRD Program under Project No. 21-SI-003. The LLNL document release number is LLNL-JRNL-832950. The authors would like to thank Rich Shuttlesworth, Glenn Huete, and Selim Elhadj for their help with preliminary measurements, test preparations, and helpful discussions. The test facility was funded by the Aeronautics Evaluation and Test Capabilities (AETC) and the Hypersonic Technology Project (HTP) of the National Air and Space Administration, Langley Research Center. The authors would like to thank our test engineers and staff, Sheila Wright, Kevin Hollingsworth, Anthony Robbins, Jonathan Crider, Paul Tucker, and Donald Day for their assistance with wind-tunnel testing. The authors would also like to thank Paul Danehy and Neil Rodrigues for supporting laser setup and safety permits, Stephen Jones for help with the schlieren system setup, Mark Kulick for help with hardware fabrication, and William Ripley for designing and setting up the optomechanical supports.

[1] D. Pieris, T. Stratoudaki, Y. Javadi, P. Lukacs, S. Catchpole-Smith, P. D. Wilcox, A. Clare, and M. Clark, Laser induced phased arrays (LIPA) to detect nested features in additively manufactured components, Mater. Des. **187**, 108412 (2020).

[2] K. J. Harke, N. Calta, J. Tringe, and D. Stobbe, Laser-based ultrasound interrogation of surface and sub-surface features in advanced manufacturing materials, Sci. Rep. **12**, 1 (2022).

[3] P. Dryburgh, R. J. Smith, P. Marrow, S. J. Lain'e, S. D. Sharples, M. Clark, and W. Li, Determining the crystallographic orientation of hexagonal crystal structure materials with surface acoustic wave velocity measurements, Ultrasonics **108**, 106171 (2020).

[4] G. Davis, R. Nagarajah, S. Palanisamy, R. A. R. Rashid, P. Rajagopal, and K. Balasubramaniam, Laser ultrasonic inspection of additive manufactured components, Int. J. Adv. Manuf. Technol. **102**, 2571 (2019).

[5] L. Ambrozinski, J. Mrowka, M. O'Donnell, and I. Pelivanov, Detection and imaging of local ply angle in carbon fiber reinforced plastics using laser ultrasound and tilt filter processing, Composites, Part A **126**, 105581 (2019).

[6] J.-F. Vandenrijt, F. Languy, C. Thizy, and M. P. Georges, in *Fifth International Conference on Optical and Photonics Engineering*, Vol. 10449 (SPIE, 2017), pp. 299–307.

[7] S. J. Davies, C. Edwards, G. S. Taylor, and S. B. Palmer, Laser-generated ultrasound: Its properties, mechanisms and multifarious applications, J. Phys. D: Appl. Phys. **26**, 329 (1993).

[8] T. W. Murray and J. W. Wagner, in *Review of Progress in Quantitative Nondestructive Evaluation*, edited by D. O. Thompson, D. E. Chimenti (Springer US, Boston, MA, 1998), Vol. 17A, pp. 619–625.

[9] J.-P. Monchalin, Optical detection of ultrasound, IEEE Trans. Ultrason. Ferroelectr. Freq. Control **33**, 485 (1986).

[10] G. Wissmeyer, M. A. Pleitez, A. Rosenthal, and V. Ntziachristos, Looking at sound: Optoacoustics with all-optical ultrasound detection, Light: Sci. Appl. **7**, 53 (2018).

[11] J.-D. Aussel and J.-P. Monchalin, Precision laser-ultrasonic velocity measurement and elastic constant determination, Ultrasonics **27**, 165 (1989).

[12] R. D. Huber, D. J. Chinn, O. O. Balogun, and T. W. Murray, High frequency laser-based ultrasound, AIP Conf. Proc. **820**, 218 (2006).

[13] S. Everton, P. Dickens, C. Tuck, and B. Dutton, Using laser ultrasound to detect subsurface defects in metal laser powder bed fusion components, JOM **70**, 378 (2018).

[14] J. Monchalin, Laser-Ultrasonics: From the Laboratory to Industry, AIP Conf. Proc. **700**, 3 (2004).

[15] C. B. Scruby and B. C. Moss, Non-contact ultrasonic measurements on steel at elevated temperatures, NDT&E Int. **26**, 177 (1993).

[16] D. R. Tenney, W. B. Lisagor, and S. C. Dixon, Materials and structures for hypersonic vehicles, J. Aircr. **26**, 953 (1989).

[17] D. Glass, in *15th AIAA International Space Planes and Hypersonic Systems and Technologies Conference* (American Institute of Aeronautics and Astronautics, Dayton, Ohio, 2008).

[18] M. Kalms, O. Focke, and C. v Kopylow, in *Ninth International Symposium on Laser Metrology*, (SPIE, 2008), Vol. 7155, pp. 128–138.

[19] A. Bounitch, D. Lewis, and J. Lafferty, in *49th AIAA Aerospace Sciences Meeting Including the New Horizons Forum and Aerospace Exposition* (American Institute of Aeronautics and Astronautics, Orlando, Florida, 2011).

[20] M. Semper, B. Pruski, and R. Bowersox, in *50th AIAA Aerospace Sciences Meeting Including the New Horizons Forum and Aerospace Exposition 2012*, Vol. 13 (American

Institute of Aeronautics and Astronautics, Nashville, Tennessee, 2012).

[21] K. T. Berger, K. E. Hollingsworth, S. A. Wright, and S. J. Rufer, in *53rd AIAA Aerospace Sciences Meeting* (American Institute of Aeronautics and Astronautics, Kissimmee, Florida, 2015).

[22] J. Everhart, in *42nd AIAA Thermophysics Conference* (2011), pp. 3480.

[23] I. Pelivanov, T. Buma, J. Xia, C.-W. Wei, and M. O'Donnell, A new fiber-optic non-contact compact laser-ultrasound scanner for fast non-destructive testing and evaluation of aircraft composites, J. Appl. Phys. **115**, 113105 (2014).

[24] I. Pelivanov, T. Buma, J. Xia, C.-W. Wei, and M. O'Donnell, NDT of fiber-reinforced composites with a new fiber-optic pump–probe laser-ultrasound system, Photoacoustics **2**, 63 (2014).

[25] See Supplemental Material at http://link.aps.org/supplemental/10.1103/PhysRevApplied.18.044062 for Details about the Experimental and Post-Processing Methods, Additional Optical Measurements without Flow, and Recordings from Piezo Tranducer Detection. (n.d.).

[26] J. Krautkrämer and H. Krautkrämer, *Ultrasonic Testing of Materials* (Springer Science & Business Media, Berlin, 2013).

[27] I. Pelivanov and M. O'Donnell, Imaging of porosity in fiber-reinforced composites with a fiber-optic pump–probe laser-ultrasound system, Compos. Part Appl. Sci. Manuf. **79**, 43 (2015).

[28] J. C. Lazaro, in *2002 IEEE Ultrasonics Symposium, 2002. Proceedings* (2002), Vol. 1, pp. 777–780.

[29] M. F. Wahab and T. C. O'Haver, Wavelet transforms in separation science for denoising and peak overlap detection, J. Sep. Sci. **43**, 1998 (2020).

[30] S. Mallat, *A Wavelet Tour of Signal Processing: The Sparse Way*, 2nd ed. (Academic Press, San Diego, 2011).

[31] D. L. Donoho and I. M. Johnstone, Adapting to unknown smoothness via wavelet shrinkage, J. Am. Stat. Assoc. **90**, 1200 (1995).

[32] D. L. Donoho, De-noising by soft-thresholding, IEEE Trans. Inf. Theory **41**, 613 (1995).

[33] F. Ykhlef, M. Arezki, A. Guessoum, and D. Berkani, in *2004 IEEE International Conference on Industrial Technology, 2004. IEEE ICIT '04* (2004), Vol. 3, pp. 1422–1425.

[34] S. G. Chang, B. Yu, and M. Vetterli, Adaptive wavelet thresholding for image denoising and compression, IEEE Trans. Image Process. **9**, 1532 (2000).

[35] B. Molavi, A. Sadr, and H. A. Noubari, in *2007 IEEE International Conference on Signal Processing and Communications* (2007), pp. 209–212.

[36] X. Chen and J. Li, Noise reduction for ultrasonic Lamb wave signals by empirical mode decomposition and wavelet transform, J. Vibroengineering **15**, 3 (2013).

[37] E. Pardo, S. J. L. Emeterio, M. A. Rodriguez, and A. Ramos, Shift invariant wavelet denoising of ultrasonic traces, Acta Acust. Acust. **94**, 685 (2008).

[38] Y. Luo, W. Xue, and Y. Yu, in *2018 37th Chinese Control Conference (CCC)* (2018), pp. 4363–4367.

[39] X.-P. Zhang and M. D. Desai, Adaptive denoising based on SURE risk, IEEE Signal Process. Lett. **5**, 265 (1998).

[40] D. L. Donoho and I. M. Johnstone, Ideal spatial adaptation by wavelet shrinkage, Biometrika **81**, 425 (1994).

[41] *Nondestructive Testing Handbook, Second Edition: Volume Seven, Ultrasonic Testing*, edited by P. McIntire, A. Birks, and R. Green, Jr. (American Society for Nondestructive Testing, Columbus, 1991), 2nd ed., Vol. 7.